

# Simulations of Nonphotochemical Hole-Burned Spectra: Dispersive Kinetics

In-Ja Lee

Department of Chemistry, College of Natural Science, Dongguk University, Kyongju-si, Kyongpook 780-714, Korea  
Received November 4, 1996

Spectral hole burning spectroscopy has been the subject of considerable research for last two decades.<sup>1-5</sup> The increase in these activity was mainly stimulated by the fact that spectral hole burning can not only provide information on relaxation processes but also is applicable to be applied to the optical memory storage.

Generally, the hole spectra are complex due to zero-phonon hole (ZPH), real- and pseudo-phonon sideband hole (PSBH), antihole and vibronic holes. The theoretical studies of hole spectra have been carried out mainly in two different ways. One is the study of hole growth<sup>6-8</sup> which is concentrated on the understanding of the effect of zero-phonon transition and dispersive kinetics. The dispersive kinetics stems from the inherent structural disorder of the amorphous solid matrix. However, this investigation has some difficulties in describing the hole spectra burned at longer burn times and/or in samples with larger Huang-Rhys factor because in these cases the hole spectra are largely affected by the phonon transitions. The other is the study of the hole profiles.<sup>9-12</sup> Since this study does not consider the effect of the dispersive kinetics but considers the effect of sider zero-phonon and multi-phonon transitions, the hole depths at burn frequency cannot be quantitatively described.

Very recently, we developed a pseudo-3-level system model to explain the hole spectra burned at arbitrary burn intensities.<sup>13</sup> It showed that the hole growth curves calculated using this model are in good agreement with the published experimental data. In this paper, the hole burned spectra are theoretically studied using the pseudo-3-level system model combined with dispersive kinetics and mean phonon frequency ( $\bar{\nu}_m$ ) approximation. The simulated hole profiles have been compared with the experimental results of 5-, 10-, 15-, 20-tetraphenyl porphyrin (TPP) in polystyrene and oxazine 720 in glycerol.

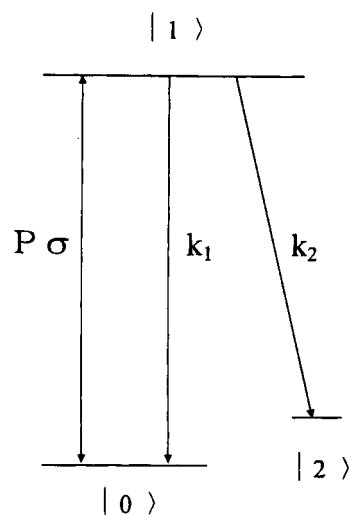
## Analysis of hole profiles

Figure 1 represents the pseudo-3-level system model. Following a burn at  $\bar{\nu}_B$  with photon flux  $P$  for a burn time  $\tau$ , the probability of sites absorbing light at  $\bar{\nu}$  through zero-phonon transition is expressed as<sup>13</sup>

$$N_r(\bar{\nu} - \bar{\nu}_m) = N_{i0}(\bar{\nu} - \bar{\nu}_m)/N \exp[-P\sigma\tau k_1 \Phi_{HB}/(2P\sigma + k_1)] \quad (1)$$

Here,  $\sigma$  is the absorption cross section,  $k_1$  is the decay rate of singlet excited state, and  $\Phi_{HB}$  is the hole burning quantum yield. And  $N_{i0}(\bar{\nu} - \bar{\nu}_m)/N$  is the zero-phonon site excitation distribution function (SDF) at  $\bar{\nu}$  before burning a hole, where  $\bar{\nu}_m$  is the central frequency of SDF.

The hole-burned absorption spectrum is expressed by the convolution of SDF (1) and the single-site absorption profile:



**Figure 1.** A 3-level hole burning kinetic model. Three level system consists of the ground state  $|0\rangle$ , excited siglet state  $|1\rangle$  and hole state  $|2\rangle$ . Hole is produced from  $|1\rangle$ .

$$A_f(\Omega) = \sum_{r=0}^{\infty} (S^r e^{-S}/r!) \int d\nu N_{i0}(\bar{\nu} - \bar{\nu}_m)/N \times l_r(\Omega - \bar{\nu} - r\omega_m) \times \exp[-P\sigma\tau\phi \times (\sum_{r=0}^{\infty} S^r e^{-S}/r! l_r(\bar{\nu}_B - \bar{\nu} - r\omega_m))/(2P\sigma + k_1)]$$

In describing the single-site absorption profile, the mean phonon frequency ( $\omega_m$ ) approximation<sup>14</sup> was utilized. Here,  $\bar{\nu}$  is zero-phonon transition frequency,  $\bar{\nu}_B$  is burn frequency,  $r$  is 0-, 1-, 2-, ..., phonon process,  $S$  is Huang-Rhys factor, and  $l_r$  is the shape of phonon transition. By considering the dispersive kinetics, which is known to be very important for nonphotochemical hole burning (NPHB), the above equation can be converted into

$$A_f(\Omega) = (2\pi\sigma_2)^{-1/2} \sum_{r=0}^{\infty} (S^r e^{-S}/r!) \int d\nu N_{i0}(\bar{\nu} - \bar{\nu}_m)/N \times \int d\lambda \exp[-(\lambda - \lambda_0)^2/2\sigma_2^2] \times l_r(\Omega - \bar{\nu} - r\omega_m) \times \exp[-P\sigma\tau\phi(\lambda) (\sum_{r=0}^{\infty} S^r e^{-S}/r! l_r(\bar{\nu}_B - \bar{\nu} - r\omega_m))/(2P\sigma + k_1)] \quad (2)$$

Here,  $\lambda_0$  and  $\sigma_2$  are average value and standard deviation of the tunnel parameter for the hole burning.

The calculated hole-burned spectra reported below were obtained by numerical integration of Eq. (2) using Bode's approximation. A Lorentzian with FWHM  $\gamma$  was employed for the zero-phonon transition and a Lorentzian with a width of  $r^{1/2}\Gamma$  for the shape of the  $r$ -phonon profile  $l_r$ . Here,  $\gamma$  is a homogeneous linewidth and  $\Gamma$  is a one-phonon width. A Gaussian for the SDF is a physically reasonable choice

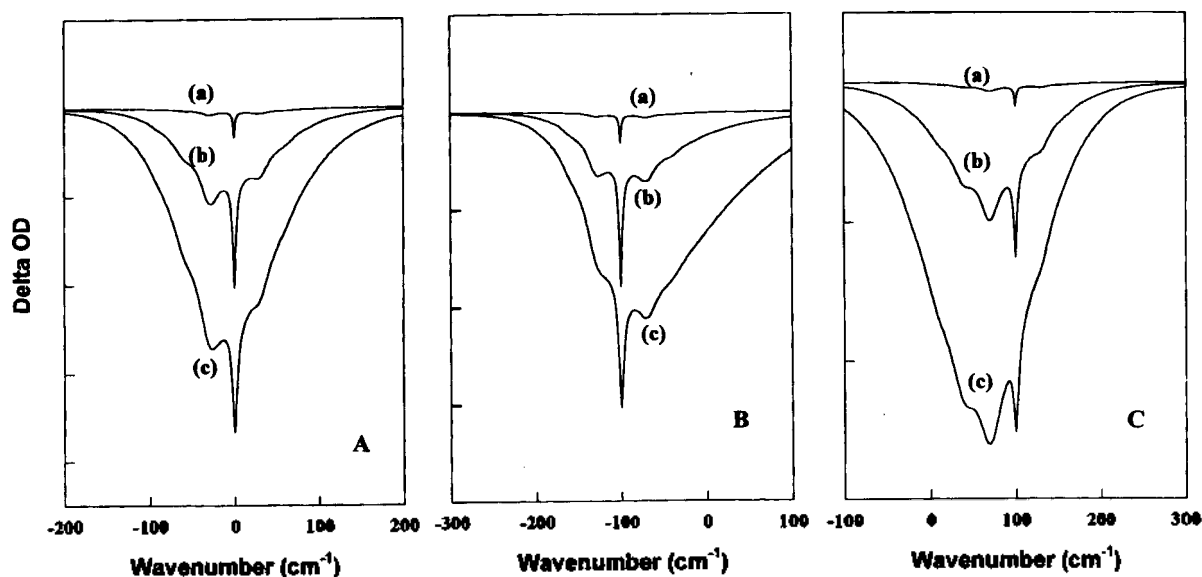


**Figure 2.** Hole-burned spectra as a function of burn time calculated using Eq. (2) for burn wavenumbers of (A)  $\bar{\nu}_m = 0.0 \text{ cm}^{-1}$ , (B)  $\bar{\nu}_m = -100 \text{ cm}^{-1}$ , and (C)  $\bar{\nu}_m = +100 \text{ cm}^{-1}$ . The burn times are (a) 25  $\mu\text{s}$ , (b) 100  $\mu\text{s}$ , (c) 1 ms, and (d) 10 ms. The parameters used are  $S=1.0$ ,  $\omega_m=30 \text{ cm}^{-1}$ ,  $\gamma=1.0 \text{ cm}^{-1}$ ,  $\Gamma=20 \text{ cm}^{-1}$ ,  $\Gamma_r=200 \text{ cm}^{-1}$ ,  $\sigma=4.0 \times 10^{-11} \text{ cm}^2$ ,  $I=68.2 \text{ mW/cm}^2$ ,  $\lambda_0=7.2$ , and  $\sigma_2=1.0$ .

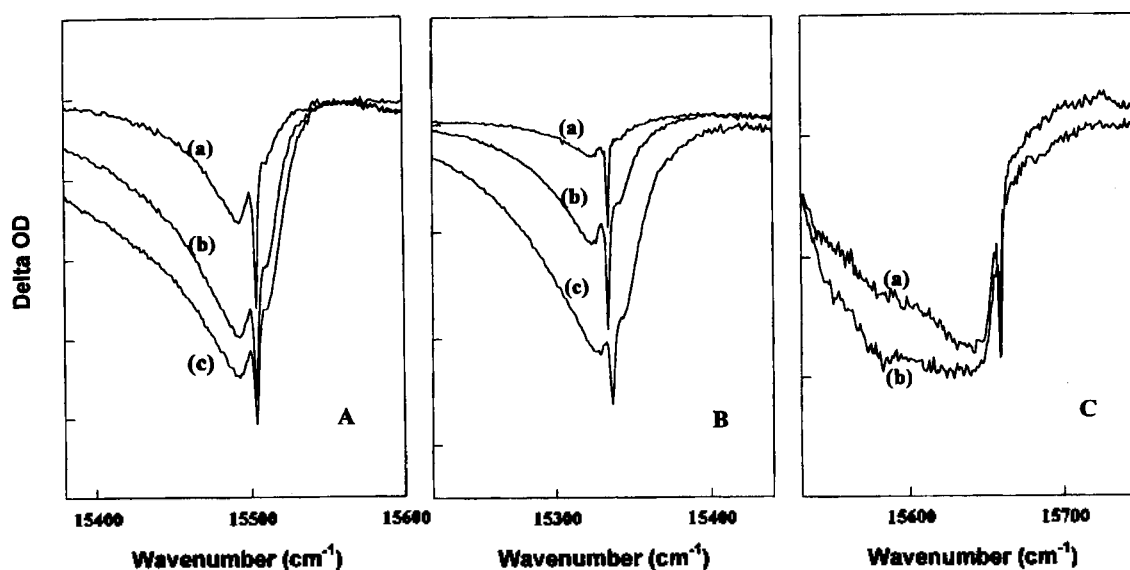


**Figure 3.** Hole spectra of 5-, 10-, 15-, 20-tetraphenyl porphyrin in polystyrene film at 4.6 K. The hole-burned spectra in (A) are obtained for  $\lambda_b=645 \text{ nm}$  and  $I_b=20 \text{ mW/cm}^2$  with burn times of (a) 15 s, (b) 5 min, and (c) 35 min. (B) is obtained for  $\lambda_b=638 \text{ nm}$  and  $I_b=20 \text{ mW/cm}^2$  with burn times of (a) 15 s, (b) 5 min, and (c) 35 min. (C) is obtained for  $\lambda_b=652 \text{ nm}$   $I_b=10 \text{ mW/cm}^2$  with burn times of (a) 1 min and (b) 11 min.

for  $N_0$ . For the Huang-Rhys factor employed, the sufficient accuracy was obtained by truncating the series at  $r=10$ . For simplicity, it is assumed that the effects of hole filling processes and polarization of light are negligible in this calculation.

### Results and Discussion

Figure 2A shows a series of hole spectra calculated as a function of burn time for the case where the burn wavenumber is equal to  $\bar{\nu}_m$ . The values of parameters used in the calculation are given in the figure caption. The hole depth scales for all the spectra in Figure 2A are the same

and the relative hole depths for ZPHs of spectra (a), (b), (c) and (d) are approximately 6, 14, 38 and 68%, respectively. The intensity of pseudo-PSBH is slightly larger than that of real-PSBH for shorter burn times. For longer burn times this becomes comparable to real-PSBH while, at the same time, the intensity ratio of pseudo-PSBH depth to the ZPH depth gets larger. These observations can be explained as follows: for shorter burn times, the sites absorbing burn beam through zero-phonon transition play an important role in the ZPH formation resulting in a ZPH accompanied by the pseudo-PSBH. As burn time increases, however, the sites absorbing the light through their phonon transitions gets deeply involved in the ZPH formation leading to the

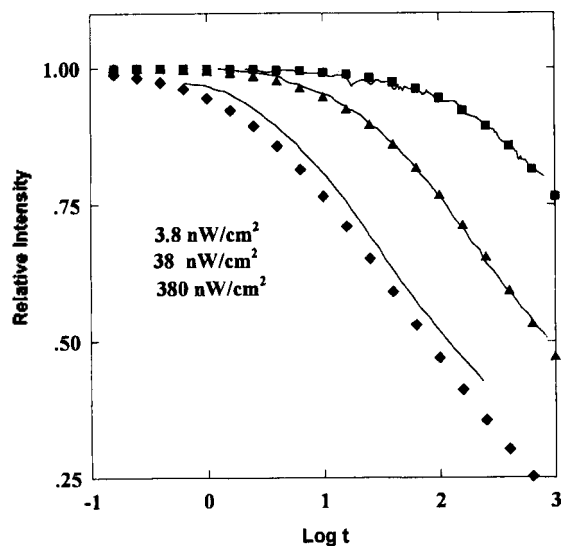


**Figure 4.** Hole growth curves for oxazine 720 in a glycerol glass as a function of  $\log t$  scale. Solid curves are experimentally obtained from ref. 14 while symbols are theoretical fits obtained with  $\lambda_0=6.8$ , and  $\sigma_2=0.8$ . The parameter values used are  $S=0.45$ ,  $\omega_m=27 \text{ cm}^{-1}$ ,  $\gamma=1.0 \text{ cm}^{-1}$ ,  $\Gamma=20 \text{ cm}^{-1}$ ,  $\Gamma_1=200 \text{ cm}^{-1}$ ,  $\sigma=4.0 \times 10^{-11} \text{ cm}^2$ ,  $\Omega_0=1.0 \times 10^{12} \text{ s}^{-1}$ , and  $k_1=3.7 \times 10^8 \text{ s}^{-1}$ .

broadening of ZPH and increasing real-PSBH.

Figure 2B and C show the hole-burned spectra calculated for  $\nu_B=\bar{\nu}_m-100 \text{ cm}^{-1}$  and  $\nu_B=\bar{\nu}_m+100 \text{ cm}^{-1}$ , respectively. The values for the parameters used in the calculation are the same with those of corresponding parameters used for Figure 2A. From the comparison of Figure 2B and 2C with 2A, it is clear that there is a pronounced dependence of the hole profile on  $\nu_B$ . The fact that the centroids of the hole profile for the longest burn times in Figure 2B and 2C are shifted about  $50 \text{ cm}^{-1}$  to the red and blue of  $\nu_B$  agrees with the previous studies.<sup>12</sup> This can be qualitatively explained by noting that as  $\nu_B$  is tuned into the high- and low-energy side of the absorption spectrum, the ratio between zero-phonon and multi-phonon ( $r \geq 1$ ) excitation will increase and decrease to give rise to hole spectra whose centroid is red and blue shifted, respectively.

To test the validity of the calculations, the simulated hole-burned spectra have been compared with the experimental results.<sup>15</sup> Figure 3 represents a series of hole burned spectra for TPP in polystyrene films at 4.6 K. The absorption maximum of TPP in polystyrene at 4.6 K is located at 645 nm (FWHM=350  $\text{cm}^{-1}$ ). Figure 3A is obtained for  $\lambda_B=645 \text{ nm}$  while Figure 3B and 3C for 652 and 638 nm, respectively.<sup>15</sup> The deepest hole depths at burn wavenumbers are (A) 16% for  $\lambda_B=645 \text{ nm}$ , (B) 22% for  $\lambda_B=638 \text{ nm}$ , and (C) 15% for  $\lambda_B=645 \text{ nm}$ , respectively. Since hole burning is photochemical for this system, antihole is distributed over the broad original inhomogeneous absorption. Therefore, the interference of the antihole with the real- and pseudo-phonon sideband is minimized. However, although contribution of NPHB is not important in this system, it is operative in the hole formation and becomes significant as the burn time increases. Because NPHB produces antihole distributed mainly on the higher energy side of the burn frequency, the observed depth of real-PSBH seems smaller than that of cal-

culated spectra. The comparison of Figure 2 with Figure 3 indicates that the TPP in polystyrene qualitatively behaves in accord with the basic predictions of the theory. The present theory explained the experimental data better than the previous study<sup>12</sup> which neglect the effect of dispersive kinetics.

Figure 4 shows the hole growth curves of oxazine 720 in glycerol host whose hole burning is nonphotochemical. The solid curves, experimentally obtained by Kenney *et al.*,<sup>16</sup> correspond to burn intensity of  $I_B=3.8, 38, \text{ and } 380 \text{ nW/cm}^2$  and  $T_B=1.6 \text{ K}$ . Simulations using Eq. (2), which are indicated by symbols, were obtained with  $\lambda_0=6.8$ ,  $\sigma_2=0.8$  and  $S=0.45$ . Although the burn intensity varies over two decades and fluence over about five orders of magnitude, the theoretical fits agree well with the experimental data. The experimental hole growth curve obtained for  $I_B=3.8 \text{ nW/cm}^2$  is blue shifted compared with the corresponding simulated hole growth curve. This may originate from the error in the power measurement.

In summary, the pseudo-3-level system model combined with dispersive kinetics and mean-phonon approximation is developed to explain the nonphotochemical hole-burned spectra. To test the validity of the model, the hole-burned spectra simulated using this model are compared with several experimental data. It shows that the predictions of the theory are in good agreement with the hole-burned spectra of TPP in polystyrene and oxazine 720 in glycerol.

**Acknowledgment.** This work was supported in part by Korea Science and Engineering Foundation (951-0302-018-2) and in part by the grant of Dongguk University.

## References

- Moerner, W. E. Ed., *Persistent Spectral Hole Burning: Science and Applications*; Springer-Verlag: Berlin, 1988 and references there in.
- Friedrich, J.; Haarer, D. *Angew. Chem. Int. Ed. Engl.* **1984**, *23*, 113.
- Hayes, J. M.; Small, G. J. *Chem. Phys. Lett.* **1978**, *54*, 435.
- Sokoda, K.; Maeda, M. *Chem. Phys. Lett.* **1994**, *217*, 152.
- Machida, S.; Horie, K. Kyono, O.; Yamashita, T. *J. Lumin.* **1993**, *56*, 85.
- Jankowiak, R.; Richert, R.; Bössler, H. *J. Phys. Chem.* **1985**, *89*, 4569.
- Jankowiak, R.; Small, G. J. *Science* **1987**, 618.
- Kanematsu, Y.; Shiraishi, R.; Imaoka, A.; Saikan, S.; Kushida, T. *J. Phys. Chem.* **1989**, *91*, 16579.
- Hayes, J. M.; Gillie, J. K.; Tang, D.; Small, G. J. *Biochim. Biophys. Acta* **1988**, *932*, 287.
- Friedrich, J.; Swalen, J. D.; Harrer, D. *J. Chem. Phys.* **1980**, *73*, 705.
- Sapozhnikov, M. N. *Chem. Phys. Lett.* **1987**, *135*, 398.
- Lee, I.-J.; Hayes, J. M.; Small, G. J. *J. Phys. Chem.* **1989**, *91*, 3463.
- Lee, I.-J. *J. Kor. Chem. Soc.* **1995**, *10*, 763.
- Pryce, M. H. L. In *Phonons in Perfect Lattices and Lattices with Point Defects*; Stevenson, R. W. H., Ed.; Oliver and Boyd: London, England, 1968; p 403.
- Lee, I.-J.; Small, G. J. unpublished result.
- Kenney, M. J. Ph. D. Dissertation, Iowa State University, Ames, Iowa, 1990.